

# Direct Electrochemistry of Catalase Immobilized at Polymerized-SnO<sub>2</sub> Multiporous Modified Electrode for an Amperometric H<sub>2</sub>O<sub>2</sub> Biosensor



Samiul Alim, Jaya Vejayan and AKM Kafi\*

Faculty of Industrial Sciences & Technology, University Malaysia Pahang, Malaysia

Received: March 16, 2018; Published: April 10, 2018

\*Corresponding author: AKM Kafi, Faculty of Industrial Sciences & Technology, University Malaysia Pahang, Kuantan 26300, Malaysia; Tel: 609 549 2392; Fax: 609 549 2766; Email: kafiakm@ump.edu.my

## Abstract

A novel amperometric H<sub>2</sub>O<sub>2</sub> biosensor based on immobilization of catalase with polymerized MPNFs of SnO<sub>2</sub> onto glassy carbon electrode with chitosan have been proposed in this work. Multiporous nanofibers of SnO<sub>2</sub> were synthesized by electrospinning method from the tin precursor by controlling the concentration followed by polymerized with aniline. Catalase was then co-immobilized with the polymerized nanofibers on the surface of glassy carbon electrode by using chitosan. The polymerized MPNFs of SnO<sub>2</sub> play a significant role in facilitating the electron exchange between the electroactive center of catalase and the electrode surface. Cyclic Voltammetry and amperometry were used to study and optimize the performance of the fabricated H<sub>2</sub>O<sub>2</sub> biosensor. The PANI/SnO<sub>2</sub>-NFs/Catalase/Ch/GCE biosensor displayed a linear amperometric response towards the H<sub>2</sub>O<sub>2</sub> concentration range from 10 to 120 μM with a detection limit of 0.6 μM (based on S/N=3). Furthermore, the biosensor reported in this work exhibited acceptable stability, reproducibility, and repeatability.

**Keywords:** Catalase; SnO<sub>2</sub>; Polyaniline; H<sub>2</sub>O<sub>2</sub> Sensing

**Abbreviations:** CV: Cyclic Voltammetric; PVP: Polyvinylpyrrolidone; DMF: Dimethylformamide; HCl: Hydrochloric Acid; NaOH: Sodium Hydroxide

## Introduction

H<sub>2</sub>O<sub>2</sub> is engendered by normal cellular metabolism as a signaling molecule for signal transduction, second messengers and growth factors [1,2]. Moreover, H<sub>2</sub>O<sub>2</sub> can pierce freely into almost any cellular compartments through membranes, and it can induce oxidative stress causing the deterioration of lipids, proteins, and DNA, as well as some diseases ranging from cancer to neurodegenerative disorder like Parkinson's or Alzheimer disease [3-5]. H<sub>2</sub>O<sub>2</sub> also has application in various fields like pharmaceutical, food and environmental analysis [6-8]. Therefore, the selective detection of H<sub>2</sub>O<sub>2</sub> is essential and numerous methods have been proposed for the last decades to ensure the reliable and fast detection of H<sub>2</sub>O<sub>2</sub> such as colorimetry [9], fluorescence [10], chemiluminescence [11], electron spin resonance [12], electrochemical biosensing [13], etc., whereas, electrochemical biosensing is the most attractive choice [14].

In the promptly progressing area of biosensors, clamping bio molecules with complex molecular structure with transducer devices is the most crucial issue to resolve for researchers [15,16]. The passage of electrons is the major drawback in direct electron transfer between these unconventional partners, whereas, effective

electrical contact between the active site of an enzyme/protein and the electrode surface is the cornerstone of any amperometric biosensor [17]. The active redox sites of enzymes/proteins are buried deeply within the insulated shell of the immobilized protein and thus in the far distance from the surface of electrode [18,19]. Numerous studies have been conducted till now to accelerate the direct electron transfer. Immobilization of the enzymes on different substrates like nonmaterial is one of the most effective ways [20]. Being inspired by the distinctive features of nanostructured materials like regular structure, excellent chemical and thermal stability, different types of nonmaterial-based biosensors have secured much attention for their uses in the health and environment.

One of the most striking nanostructured materials is tin oxide (SnO<sub>2</sub>) which has been used as nanotubes, nanoparticles, nanowires, and nanorods [21,22]. Nanostructured SnO<sub>2</sub> possesses high surface area, nontoxicity, excellent biocompatibility, catalytic activity and chemical stability [23] which makes it suitable for various applications such as solar cells, electrochemistry, and biosensor [24-26]. We have fabricated a new one-dimensional nano-morphology of SnO<sub>2</sub> recently with the higher surface area and

enhanced electron mobility characteristics, named as multiporous nanofibers (MPNFs). It was synthesized through electrospinning method by controlling the tin precursor concentration [27]. This potential nanofiber can be transcended in contrast with other conventional nanofibers and nanowires if used in biosensing. Moreover, incorporation of a polymer such as polyaniline (PANI) with this nanofiber can intensify its electrical conductivity along with some other characteristics like mechanical flexibility, thermal and chemical stability [28,29] which can be an incentive for the advancement of the biosensor.

Catalase is a heme-containing homotetrameric enzyme can resist the accumulation of  $H_2O_2$  and fortifies cellular organelles and tissues from the damage caused by peroxide. This enzyme has been extensively used in biosensor and selective determination of  $H_2O_2$  [30,31]. In this work, we have developed a new electrode modified with the organization of Polyaniline- $SnO_2$  NF-catalase enzyme on glassy carbon electrode by using chitosan. Followed by the synthesis of  $SnO_2$  NF, polyaniline (PANI) has been polymerized on  $SnO_2$  to develop  $SnO_2$ -PANI composite. The proposed modified electrode was then applied for  $H_2O_2$  biosensing. To the best of our knowledge for the first time, polymerized multiporous nanofibers of  $SnO_2$  and chitosan composite has been used to study direct electrochemistry of catalase enzyme and used in selective and reliable detection of  $H_2O_2$ .

## Experimental

### Reagents and Materials

Tin chloride pentahydrate ( $SnCl_4 \cdot 5H_2O$ ), polyvinylpyrrolidone (PVP) and dimethylformamide (DMF) were bought from Sigma. Catalase, chitosan and a stock solution of  $H_2O_2$  (30 wt %) were also purchased from Sigma and used as received and preserved at 4°C. Aniline monomer (99.5%) and ammonium persulfate (APS, 98%) were obtained from E. Merck (Germany). The pure water (18 M $\Omega$ . cm) used to prepare all solutions in this work was purified with the Nanopure<sup>®</sup> water system. All other reagents were of analytical grade, and 0.01 M Phosphate buffer of pH 7.0 was freshly prepared every time before use. 1.0 M hydrochloric acid (HCl) or 1.0 M sodium hydroxide (NaOH) was used in order to procure the desired pH of phosphate buffer.

### Fabrication of the $SnO_2$ Nanofiber

Multiporous  $SnO_2$  nanofiber was fabricated according to the procedure described in our previous work [26]. To sum up, the starting reagents were tin chloride pentahydrate ( $SnCl_4 \cdot 5H_2O$ ), polyvinylpyrrolidone (PVP), dimethylformamide (DMF) and ethanol, whereas, 3 g of PVP was dissolved in an equal volume ratio (1:1) of ethanol and DMF and different concentrations of the tin precursor were dissolved to this solution at room temperature until the solution become transparent. The concentrations of tin precursor used in fabrication were 5.5mM, 7mM, 8.5mM, 10mM, 11.5mM and were labeled as C0, C1, C2, C3 and C4, respectively. For electrospinning, the viscosity of the solution was measured with a rheometer (LVDV III Ultra, Brook<sup>®</sup> eld Co., USA) and the solutions were then transferred to a plastic syringe with steel needles and the procedure was operated by the following parameters:

- applied voltage, 25 kV,
- The injection rate, 0.6 mL h<sup>-1</sup>,
- The distance between the collector and the tip of the needle, 20cm
- Humidity, 40-45%, and
- 1200 rpm speed of the rotating collector. Solid nanofibers were then collected from the collector and annealed at 600 °C temperature for 3 hour at heating rate 0.5 °C per minute.

### Synthesis of Polyaniline (PANI) and PANI- $SnO_2$ -NFs

Followed by the fabrication of  $SnO_2$ -NFs, polyaniline (PANI) has been polymerized on  $SnO_2$  using chemical oxidation polymerization method to construct PANI- $SnO_2$ -NF composite [32]. For the synthesis of polyaniline, Aniline (0.1M) and ammonium persulphate (0.1M) were dissolved separately in 0.1 M HCl solution and stirred for 1 h. 5mL of HCL (0.1M) and 5 mL of 0.1 M aniline monomer were then mixed in 1:1 ratio. 5% solution of oxidant APS prepared in 0.1 M HCl was added dropwise to the above mixture until well-dispersed solution by keeping the temperature about 0-5 °C under continuous stirring. After 3 h, a reasonable degree of polymerization (a greenish black precipitate) was obtained. The precipitate produced in the reaction was separated by filtration, repeatedly washed with distilled water until the pH reached at 7.0 and dried under vacuum for 24 h.

$SnO_2$  nanofibers (30mg) were suspended individually in 0.1 M HCl (13 mL) solution and sonicated for 1 h to minimize aggregation of  $SnO_2$  nanofibers. 10 mL aniline (in 0.1 M HCl) solution and 10 mL  $SnO_2$  nanofibers suspension were mixed and further sonicated for 30 min. 10mL APS solution was then slowly added dropwise to well-dispersed suspension mixture with vigorously continuous stirring at 0-5 °C. The mixture colour turns to greenish after adding APS and stirrer is continued to about 5 h. The mixture was then kept overnight to settle the precipitate. A good degree of composite polymerization was perceived after that. The precipitate was washed on the next day with distilled water for several times until pH 7.0, dried in the vacuum oven at 60 °C for 3 h before it was pounded to powder.

### Fabrication of Biosensor

A stock solution of 10 mg of PANI/ $SnO_2$  NF was prepared in 100 $\mu$ l phosphate buffer, and the stock solution of 2 mg/ml of catalase was made in phosphate buffer (pH 7.0). A glassy carbon electrode (3 mm of diameter) was polished with alumina powder (0.05 $\mu$ M), rinsed thoroughly with deionized water and acetone subsequently, and then dried at room temperature. Finally, 5 $\mu$ L of PANI/ $SnO_2$  NF the stock solution and 5 $\mu$ L of catalase from the stock solution were co-immobilized onto the glassy carbon electrode together with 2 $\mu$ L of 2mg/ml of chitosan (Ch). The electrodes used for comparison were fabricated in the same way with only  $SnO_2$  NF and only catalase. All the resulting electrodes are denoted as PANI/ $SnO_2$ NF/Catalase/Ch/GC, PANI/ $SnO_2$ NF/Ch/GC and Catalase/Ch/GC respectively. All the electrodes were stored at 4 °C in 0.1 M phosphate buffer at pH 7.0 when not in use.

## Morphological and Electrochemical Characterization

Morphological characterization of synthesized nanofiber was evaluated by field emission scanning electron microscopy (JEOL-USA). The electrochemical measurements were carried out by using Potentiostat PARSTAT 2273 on a CHI (630B) workstation. A three-electrode system was employed, whereas, a modified electrode as the working electrode, a platinum wire as a counter electrode and an Ag/AgCl was used as reference electrode. Cyclic voltammetric (CV) measurements were carried out in 0.1 M phosphate buffer by scanning the electrode potential in the range between 0.2 and -0.6V versus Ag/AgCl. Amperometric responses were measured in 0.1 M phosphate buffer stirred by a magnetic stirrer. All electrolytes were deoxygenated before experiments by bubbling ultra-pure nitrogen for 15 min and the relative measurements were carried out at room temperature.

## Results and Discussions

### Surface characterization of multiporous SnO<sub>2</sub> Nanofiber

Field emission scanning electron microscopy (FESEM) was employed to study the morphological characteristics of the MPNFs of SnO<sub>2</sub>. Figure 1 delineates the morphology of MPNFs of SnO<sub>2</sub>. The acquired multiporous SnO<sub>2</sub> nanofiber possessed a fibrous structure according to the FESEM image in all the areas with fiber-fiber interconnections. We have already deliberated about the MPNFs of SnO<sub>2</sub> in our previous work whereas, MPNFs were fabricated with grains size of 5-15 nm and they were smaller than the grain size of the PNFs (15-25 nm) [23].

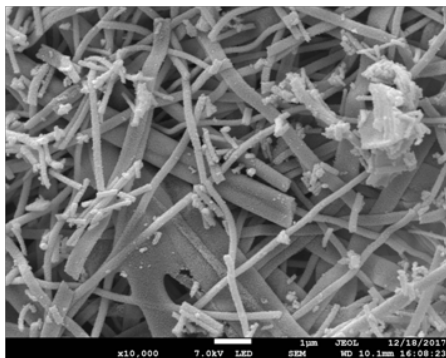


Figure 1: (a) SEM image of the MPNFs of SnO<sub>2</sub>.

### Electrochemical Measurement of the Modified Electrodes

Figure 2 elucidates the cyclic voltammograms (CVs) of the

- bare,
- PANI/SnO<sub>2</sub>-NFs/Ch/GCE;
- Catalase/Ch/GCE; and
- PANI/SnO<sub>2</sub>-NFs/Catalase/Ch/GCE electrodes recorded in a 0.1M phosphate buffer (pH 7.0) at a scan rate of 50mV/s. As expected, neither oxidation nor reduction peak appears in the CV of the bare electrode and PANI/SnO<sub>2</sub>-NFs/Ch/GCE electrode showed tiny redox peak. But a moderate reduction peak appears in the CV of the Catalase/Ch/GCE electrode.

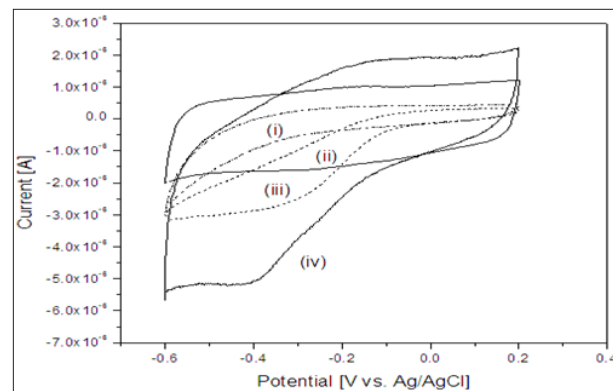
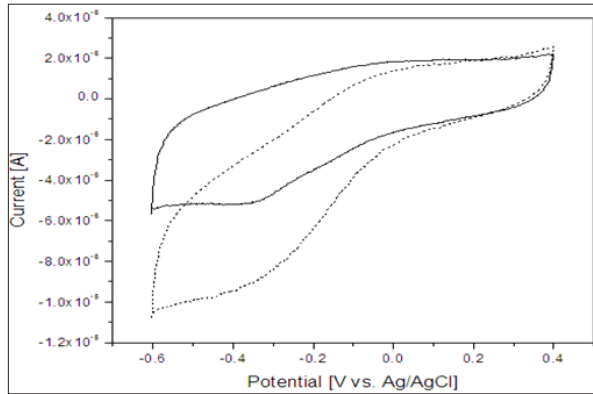


Figure 2: Cyclic voltammograms response of a. Bare GCE electrode; b. PANI/SnO<sub>2</sub>-NFs/Ch/GCE electrode; c. Catalase/Ch/GCE electrode; and d. PANI/SnO<sub>2</sub>-NFs/Catalase/Ch/GCE electrode in 0.1 M phosphate buffer at pH 7.0 at a scan rate of 50mV/s.

This cathodic peak is attributed to the reduction of HRP at the underlying electrodes. However, a well-defined oxidation and reduction peak appear in the CV of the PANI/SnO<sub>2</sub>-NFs/Catalase/Ch/GCE electrode, whereas, the anodic and cathodic peak potentials are located at -0.1 V and -0.4 V respectively. Both the anodic and cathodic current is higher than both of the PANI/SnO<sub>2</sub>-NFs/Ch/GCE and Catalase/Ch/GCE electrode. The formal potential  $E_n | E_n = (E_{pa} + E_{pc})/2$  was calculated to be -0.25 V. The information about electrochemical mechanism can be obtained from the relationship between peak current and scan rate [33]. The effect of the scan rates on the response of PANI/SnO<sub>2</sub>-NFs/Catalase/Ch/GCE electrode was evaluated. The linear enhancement of both the oxidation and reduction peak current was observed with the increase of scan rates from 50 to 140 mV/s respectively (data not shown) which suggests that the nature of redox process in the electrode was surface controlled process [33]. The peak-to-peak difference also enhances evenly with the augmentation of scan rates. The results suggest the reduction of all the electroactive redox enzymes at the PANI/SnO<sub>2</sub>-NFs/Catalase/Ch/GCE electrode on the forward cathodic scan [34].

### Electrochemical response of the PANI/SnO<sub>2</sub>-NFs/Catalase/Ch/GCE Biosensor to H<sub>2</sub>O<sub>2</sub>

Figure 3 represents the cyclic voltammograms of the PANI/SnO<sub>2</sub>-NFs/Catalase/Ch/GCE electrode recorded in the absence and presence of  $10 \times 10^{-5}$  M H<sub>2</sub>O<sub>2</sub> in 0.1M Phosphate buffer at pH 7.0 at a scan rate of 50mV/s. As shown in the figure, the PANI/SnO<sub>2</sub>-NFs/Catalase/Ch/GCE electrode gives its diffusional redox wave in the absence of H<sub>2</sub>O<sub>2</sub> in electrolyte (solid line), whereas, with the introduction of hydrogen peroxide to the solution, a sharp enhancement of cathodic current is appeared (dashed line) with a simultaneous decrease in the corresponding anodic peak. And this change indicates that the enhanced reduction current in the presence of H<sub>2</sub>O<sub>2</sub> is due to the presence of heme redox active center of immobilized catalase on the fabricated electrode. The results illustrate that the immobilized catalase possessed excellent electrocatalytic activity towards H<sub>2</sub>O<sub>2</sub> reduction.



**Figure 3:** Cyclic voltammograms response of the PANI/SnO<sub>2</sub>-NFs/Catalase/Ch/GCE electrode in the absence and presence (dashed line) of  $2.0 \times 10^{-5}$  M H<sub>2</sub>O<sub>2</sub> in 0.1M phosphate buffer at pH 7.0 at a scan rate of 50mV/s.

The impact of the applied electrode potential and pH of the phosphate buffer on the amperometric response of the PANI/SnO<sub>2</sub>-NFs/Catalase/Ch/GCE electrode was evaluated to the introduction of  $1 \times 10^{-5}$  M H<sub>2</sub>O<sub>2</sub> in 0.1M phosphate buffer at pH 7.0 on the applied potential ranging from 0.3 to -0.6V. The reduction current increased when the applied potential was decreased from 0.3 to -0.4 V. Further reducing the applied potential from -0.4V leads to the declined amperometric response. The best current response was obtained at -0.4V and therefore, the potential -0.4 V was chosen as the working potential for this biosensor. The effect of pH on the amperometric response of the PANI/SnO<sub>2</sub>-NFs/Catalase/Ch/GCE electrode was also investigated in the presence of  $1 \times 10^{-5}$  M

H<sub>2</sub>O<sub>2</sub> in 0.1M Phosphate buffer while the pH was varied from 4.0 to 10.0. The maximum reduction current was achieved at a pH of 7.0. However, a decline of reduction current is obtained when the pH is further increased from 8.0 to 10.0. The current response is very low at the lower pH values (<4.0) of electrolytes which can be caused by the denaturation of bio molecules [35-37]. Therefore, the pH 7.0 was determined as the optimal pH value of electrolyte to obtain highest current response and it corroborates the concept that the pH range of 6.0-7.5 provides the optimum environment for enzymatic electrochemical reactions [35].

### Amperometric Response of the Biosensor

The analytical property of PANI/SnO<sub>2</sub>-NFs/Catalase/Ch/GCE was further investigated by the amperometric response towards the reduction of H<sub>2</sub>O<sub>2</sub>. The amperometric response of the PANI/SnO<sub>2</sub>-NFs/Catalase/Ch/GCE electrode has been investigated by successive accretion of H<sub>2</sub>O<sub>2</sub> concentration in a stirred cell containing 0.1M phosphate buffer under the optimized pH and potential. Figure 4a shows the typical amperometric response of the PANI/SnO<sub>2</sub>-NFs/Catalase/Ch/GCE electrode for successive inclusion of H<sub>2</sub>O<sub>2</sub> and the corresponding calibration plot for the amperometric response is shown in Figure 4b. The response current strikingly increases with the increase of H<sub>2</sub>O<sub>2</sub> concentration. The response time for this fabricated electrode was very fast, reaching 95% of its maximum current response in about 5 s. The biosensor shows a linear response ranging from 10 to 120  $\mu$  M concentrations of H<sub>2</sub>O<sub>2</sub> with a correlation coefficient of 0.996 and the detection limit was determined to be 0.6  $\mu$  M (based on S/N=3).

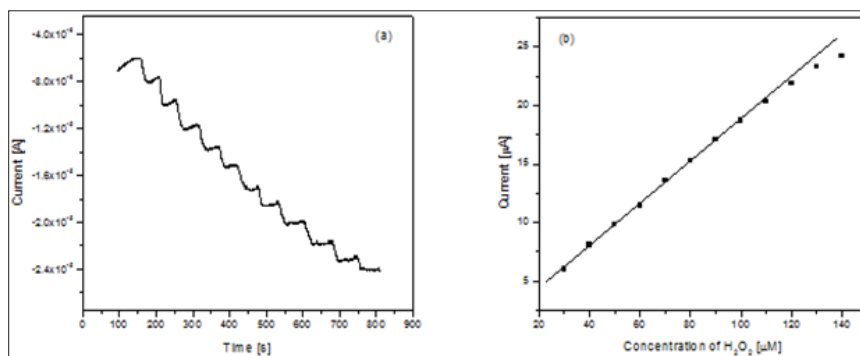


**Figure 4:**

- Amperometric response of PANI/SnO<sub>2</sub>-NFs/Catalase/Ch/GCE electrode with total addition of  $14 \times 10^{-5}$  M of H<sub>2</sub>O<sub>2</sub> in phosphate buffer at pH 7.0 at potential of -0.35 V.
- Calibration plots for the proposed PANI/SnO<sub>2</sub>-NFs/Catalase/Ch/GCE electrode.

**Table 1:** Suggests that the proposed biosensor offers satisfactory stability and acceptable reproducibility with lower detection limit.

Modified electrode	LOD	Stability	References
Hb nanoparticles onto gold electrode	1.0 $\mu$ M	90% after 90 days	[36]
Catalase on nafion and CNT composite	0.83 $\mu$ M	Not available	[37]
HRP in disposable CNT	0.85 $\mu$ M	Not available	[38]
HRP in AuNps and chicken egg shell membrane	3.0 $\mu$ M	88.6% (20 days)	
HRP in SnO <sub>2</sub> nanowires	0.8 $\mu$ M	95.3% (10 days)	[39]
HB in TiO <sub>2</sub> Nanotube arrays	2.0 $\mu$ M	95% (21 days)	[40]
Catalase with PANI/SnO <sub>2</sub> - MPNFs	0.6 $\mu$ M	92% (35 days)	This work

## Stability and Repeatability of the Biosensor

Stability and repeatability are among the most remarkable factor about any biosensor, which are ascribed on several strands. The long-term stability of this fabricated biosensor was assessed by storing the electrode in phosphate buffer (pH 7.0) at 40 C for 35 days and the electrode perpetuated 92% of its initial response to  $1 \times 10^{-5}$  M  $H_2O_2$ . The repeatability of the biosensor for current response was also evaluated and the relative standard deviation (R.S.D.) was 3.5% for 10 successive assays using the same enzyme electrode. A comparison of performances of this fabricated biosensor with other recent  $H_2O_2$  biosensors fabricated with redox enzyme/protein and different nonmaterial has been summarized in Table 1 which suggests that the proposed biosensor offers satisfactory stability and acceptable reproducibility with lower detection limit [38-40].

## Conclusion

The insight of this work has an impetus to investigate the direct electrochemistry of catalase on the electrode surface by immobilizing with the polymerized  $SnO_2$  multiporous nanofibers (MPNFs) with its application in biosensing. The results demonstrated in this study corroborates that a well-defined redox peaks are capable of being formed from redox group of catalase and the fabricated electrode exhibits a high catalytic efficiency towards  $H_2O_2$ . Amperometric experiments were executed under optimal condition (pH 7.0 and applied potential -0.4V). The modified electrode exhibited a good catalytic response to  $H_2O_2$  with a longer liner range 10-120  $\mu$ M and a LOD of 0.6  $\mu$ M. Moreover, the biosensor showed acceptable stability, reproducibility and repeatability. The overall capabilities of the fabricated biosensor indicate that it can be convenient in sensitive detection of  $H_2O_2$  with its possible application in biomedical and industry; also, the multiporous  $SnO_2$  nanofiber can be a promising nonmaterial for fabricating more advanced biosensor in future.

## Acknowledgment

University Malaysia Pahang local research grants (RDU 1703176).

## References

1. N Saha, R Schreiber, S Vom Dahl, F Lang, W Gerok, et al. (1993) Endogenous hydroperoxide formation, cell volume and cellular K<sup>+</sup> balance in perfused rat liver. *Biochemical Journal* 296(Pt 3): 701-707.
2. SG Rhee (2006)  $H_2O_2$ , a necessary evil for cell signaling. *Science* 312(5782): 1882-1883.
3. D Trachootham, J Alexandre, P Huang (2009) Targeting cancer cells by ROS-mediated mechanisms: a radical therapeutic approach? *Nature reviews Drug discovery* 8(7): 579-591.
4. NG Milton (2004) Role of hydrogen peroxide in the aetiology of Alzheimer's disease. *Drugs & aging* 21(2): 81-100.
5. N Simonian, J Coyle (1996) Oxidative stress in neurodegenerative diseases. *Annual review of pharmacology and toxicology* 36(1): 83-106.
6. K Zhou, Y Zhu, X Yang, J Luo, C Li, et al. (2010) A novel hydrogen peroxide biosensor based on Au-graphene-HRP-chitosan biocomposites. *Electrochimica Acta* 55(9): 3055-3060.
7. Z Cao, X Jiang, Q Xie, S Yao (2008) A third-generation hydrogen peroxide biosensor based on horseradish peroxidase immobilized in a tetrathiafulvalene-tetracyanoquinodimethane/multiwalled carbon nanotubes film. *Biosensors and Bioelectronics* 24(2): 222-227.
8. L Li, Z Du, S Liu, Q Hao, Y Wang, et al. (2010) A novel nonenzymatic hydrogen peroxide sensor based on  $MnO_2$ /graphene oxide nanocomposite. *Talanta* 82(5): 1637-1641.
9. CK Lim, YD Lee, J Na, JM Oh, S Her, et al. (2010) Chemiluminescence-Generating Nanoreactor Formulation for Near-Infrared Imaging of Hydrogen Peroxide and Glucose Level in vivo, *Advanced Functional Materials* 20(16): 2644-2648.
10. J Qiao, Z Liu, Y Tian, M Wu, Z Niu (2015) Multifunctional self-assembled polymeric nanoprobe for FRET-based ratiometric detection of mitochondrial  $H_2O_2$  in living cells. *Chemical Communications* 51(17): 3641-3644.
11. H Zhou, J Liu, S Zhang (2015) Quantum dot-based photoelectric conversion for biosensing applications. *TrAC Trends in Analytical Chemistry* 67: 56-73.
12. K Abbas, M Hardy, F Poulhès, H Karoui, P Tordo, et al. (2014) Detection of superoxide production in stimulated and unstimulated living cells using new cyclic nitron spin traps. *Free Radical Biology and Medicine* 71: 281-290.
13. W Chen, S Cai, QQ Ren, W Wen, YD Zhao (2012) Recent advances in electrochemical sensing for hydrogen peroxide: a review. *Analyst* 137(1): 49-58.
14. Y Zhao, D Huo, J Bao, M Yang, M Chen, et al. (2017) Biosensor based on 3D graphene-supported  $Fe_3O_4$  quantum dots as biomimetic enzyme for in situ detection of  $H_2O_2$  released from living cells. *Sensors and Actuators B: Chemical* 244: 1037-1044.
15. P Das, M Das, SR Chinnadaiyala, IM Singha, P Goswami (2016) Recent advances on developing 3rd generation enzyme electrode for biosensor applications. *Biosensors and Bioelectronics* 79: 386-397.
16. DG Rackus, MH Shamsi, AR Wheeler (2015) Electrochemistry, biosensors and microfluidics: a convergence of fields. *Chemical Society Reviews* 44(15): 5320-5340.
17. C Chen, Q Xie, D Yang, H Xiao, Y Fu, et al. (2013) Recent advances in electrochemical glucose biosensors: a review. *Rsc Advances* 3(14): 4473-4491.
18. JH Luong, JD Glennon, A Gedanken, SK Vashist (2017) Achievement and assessment of direct electron transfer of glucose oxidase in electrochemical biosensing using carbon nanotubes, graphene, and their nanocomposites. *Microchimica Acta* 184(2): 369-388.
19. A Kafi, A Ahmadalinezhad, J Wang, DF Thomas, A Chen (2010) Direct growth of nanoporous Au and its application in electrochemical biosensing. *Biosensors and Bioelectronics* 25(11): 2458-2463.
20. S Xu, X Qin, X Zhang, C Zhang (2015) A third-generation biosensor for hydrogen peroxide based on the immobilization of horseradish peroxidase on a disposable carbon nanotubes modified screen-printed electrode. *Microchimica Acta* 182(7): 1241-1246.
21. YZ Zhang, H Pang, Y Sun, WY Lai, A Wei, et al. (2013) Porous tin oxide nanoplatelets as excellent-efficiency photoelectrodes and gas sensors. *Int J Electrochem Sci* 8: 3371-3378.
22. Q Zhou, L Yang, G Wang, Y Yang (2013) Acetylcholinesterase biosensor based on  $SnO_2$  nanoparticles-carboxylic graphene-nafion modified electrode for detection of pesticides. *Biosensors and Bioelectronics* 49: 25-31.
23. Q Wali, A Fakhruddin, I Ahmed, MH Ab Rahim, J Ismail, et al. (2014) Multiporous nanofibers of  $SnO_2$  by electrospinning for high efficiency dye-sensitized solar cells. *Journal of Materials Chemistry A* 2(41): 17427-17434.
24. N Lavanya, S Radhakrishnan, C Sekar (2012) Fabrication of hydrogen peroxide biosensor based on Ni doped  $SnO_2$  nanoparticles. *Biosensors and Bioelectronics* 36(1): 41-47.

25. B Cai, W Mao, Z Ye, J Huang (2016) Facile fabrication of all-solid-state  $\text{SnO}_2/\text{NiCo}_2\text{O}_4$  biosensor for self-powered glucose detection. *Applied Physics A* 122(9): 806.
26. AKM Kafi, Q Wali, R Jose, TK Biswas, MM Yusoff (2017) A glassy carbon electrode modified with  $\text{SnO}_2$  nanofibers, polyaniline and hemoglobin for improved amperometric sensing of hydrogen peroxide. *Microchimica Acta* 184(11): 4443-4450.
27. Q Wali, A Fakharuddin, I Ahmed, MH Ab Rahim, J Ismail, (2014) Multiporous nanofibers of  $\text{SnO}_2$  by electrospinning for high efficiency dye-sensitized solar cells. *Journal of Materials Chemistry A* 2(41): 17427-17434.
28. Z Liu, J Wang, D Xie, G Chen (2008) Polyaniline-Coated  $\text{Fe}_3\text{O}_4$  Nanoparticle-Carbon-Nanotube Composite and its Application in Electrochemical Biosensing. *Small* 4(4): 462-466.
29. Q Xu, SX Gu, L Jin Ye, Zhou, Z Yang, et al. (2014) Graphene/polyaniline/gold nanoparticles nanocomposite for the direct electron transfer of glucose oxidase and glucose biosensing, *Sensors and Actuators B: Chemical* 190: 562-569.
30. SAKgöl, E Dinçkaya, (1999) A novel biosensor for specific determination of hydrogen peroxide: catalase enzyme electrode based on dissolved oxygen probe. *Talanta* 48(2): 363-367.
31. KB Obrien, SJ Killoran, RD Oneill, JP Lowry (2007) Development and characterization in vitro of a catalase-based biosensor for hydrogen peroxide monitoring. *Biosensors and Bioelectronics* 22(12): 2994-3000.
32. J Zhu, X Liu, X Wang, X Huo, R Yan (2015) Preparation of polyaniline-TiO<sub>2</sub> nanotube composite for the development of electrochemical biosensors, *Sensors and Actuators B: Chemical* 221: 450-457.
33. S Liu, Z Dai, H Chen, H Ju (2004) Immobilization of hemoglobin on zirconium dioxide nanoparticles for preparation of a novel hydrogen peroxide biosensor. *Biosensors and Bioelectronics* 19(9): 963-969.
34. A Kafi, MJ Crossley (2013) Synthesis of a conductive network of cross linked carbon nanotube/hemoglobin on a thiol-modified Au Surface and its application to biosensing. *Biosensors and Bioelectronics* 42: 273-279.
35. AS Santos, AC Pereira, MD Sotomayor, CR Tarley, N Durán, LT Kubota (2007) Determination of Phenolic Compounds Based on Co-Immobilization of Methylene Blue and HRP on Multi-Wall Carbon Nanotubes. *Electro analysis* 19(5): 549-554.
36. V Narwal, N Yadav, M Thakur, CS Pundir (2017) An amperometric  $\text{H}_2\text{O}_2$  biosensor based on hemoglobin nanoparticles immobilized on to a gold electrode. *Bioscience reports* 37(4): BSR20170194.
37. G Fusco, P Bollella, F Mazzei, G Favero, R Antiochia (2016) Catalase-based modified graphite electrode for hydrogen peroxide detection in different beverages. *Journal of analytical methods in chemistry*, p. 12.
38. S Xu, X Qin, X Zhang, C Zhang (2015) A third-generation biosensor for hydrogen peroxide based on the immobilization of horseradish peroxidase on a disposable carbon nanotubes modified screen-printed electrode. *Microchimica Acta* 182(7-8): 1241-1246.
39. L Li, J Huang, T Wang, H Zhang, Y Liu, et al. (2010) An excellent enzyme biosensor based on Sb-doped  $\text{SnO}_2$  nanowires. *Biosensors and Bioelectronics* 25(11): 2436-2441.
40. A Kafi, G Wu, A Chen (2008) A novel hydrogen peroxide biosensor based on the immobilization of horseradish peroxidase onto Au-modified titanium dioxide nanotube arrays. *Biosensors and Bioelectronics* 24(4): 566-571.



This work is licensed under Creative Commons Attribution 4.0 License

Submission Link: <https://biomedres.us/submit-manuscript.php>



#### Assets of Publishing with us

- Global archiving of articles
- Immediate, unrestricted online access
- Rigorous Peer Review Process
- Authors Retain Copyrights
- Unique DOI for all articles

<https://biomedres.us/>